

# Investigation of the Effect of Dissolved Hydrogen on the Oxide Film on Alloy 600 in High Temperature Water by In-situ Electrochemical Techniques

Qunjia Peng (member), Yoichi Takeda, Jiro Kuniya, Tetsuo Shoji (member)  
Fracture and Reliability Research Institute, Tohoku University  
6-6-01, Aramaki Aoba, Aoba-ku, Sendai City 980-8579, Japan

In order to improve the understanding of the effect of dissolved hydrogen (DH) on the property of oxide film in high temperature water, the electronic properties of the oxide film on Alloy 600 in high temperature water under various levels of DH were studied by contact electric resistance (CER) technique and electrochemical impedance spectroscopy. The results showed that the oxide film exhibited n-type semiconductivity. The film resistance, charge transfer resistance and ionic defect transport resistance were all decreased by higher on DH, suggesting that increasing DH could increase the defectiveness of the film as well as enhance the ionic defect transport in the film. The results suggest that hydrogen could affect the oxidation kinetics as well as the stability of the oxide film.

**Keywords:** Dissolved Hydrogen, High Temperature Water, Alloy 600, Oxide Film, Electronic Properties

---

## 1. Introduction

It has been well known that hydrogen in aqueous solution can be beneficial to metals, which reduces oxidizing species, decreases the corrosion potential and the oxidation rate, etc. One application of the beneficial effects of hydrogen is to light water reactors. Hydrogen is often added to high temperature water to maintain low levels of dissolved oxygen and thereby minimize the corrosion of structural metals. In the primary water of pressurized water reactors (PWRs), however, studies have shown that the dissolved hydrogen (DH) is detrimental to the stress corrosion cracking (SCC) performance of nickel-based alloys (e.g., alloys 600, 182 and X-750) [1-3], which causes a peak in crack growth rate (CGR) in proximity to the nickel (Ni) to nickel oxide (NiO) phase transition. To date, several mechanisms, including slip-dissolution/oxidation, hydrogen-assisted cracking, internal oxidation, have been proposed to describe the SCC of nickel-based alloys in high temperature, hydrogenated water [4, 5]. Since oxidation is responsible for crack advance in the slip-dissolution/oxidation and internal oxidation mechanisms and is believed to be the main source of detrimental hydrogen in a hydrogen-assisted cracking mechanism, all mechanisms are oxidation-driven mechanisms. The DH is expected

to directly affect the extent of metal oxidation, since the electrochemical potential (ECP) which is controlled by the DH often affects oxidation thermodynamics. Further, hydrogen dissolved in metals has been found to promote the oxidation from the view points of oxidation kinetics and the transport behavior of ions and vacancies in the oxide film [6, 7]. In general, the effect of DH on SCC is expected to be characterized primarily by the influence of DH on the thermodynamics and kinetics of oxidation that play a key role in oxidation-assisted cracking.

Alloy 600 is one type of nickel-based alloys that are used extensively in PWR due to its low corrosion and oxide release rates in primary and secondary coolants as well as the compatibility of its thermal expansion coefficients with that of low alloy pressure vessel steels. As stated earlier, this alloy is susceptible to primary water SCC (PWSCC) that shows DH dependent. Composition and microstructures of the film formed on the alloy in primary water have been analyzed ex-situ using micro-analytical techniques [8-10]. However, the properties of the oxide film are dependent not only on the chemical composition and microstructure, but also on the electronic properties of the film. To the authors' knowledge, systematic studies of the electronic properties of the oxide film formed on Alloy 600 in high temperature water are not much. The relationship among the structure, chemical

composition and electronic properties of films and their stability in high temperature water is still a matter of considerable debate.

In efforts to improve the understanding of the electronic properties of oxide film in high temperature water and hence to the PWSCC mechanism, effects of DH on the electronic properties of the oxide film on Alloy 600 in high temperature water were studied by a combination of the in-situ electrochemical techniques: dc electric resistance measurements by contact electric resistance (CER) technique and ac electrochemical impedance measurements by electrochemical impedance spectroscopy (EIS). The results provided informations about the stability and ionic defect transport behavior of the oxide film.

## 2. Experiment

The material used for the experiments is mill-annealed Alloy 600, whose composition and mechanical properties are listed in Table 1. Specimens used for both CER and impedance measurements are a pair of 2 mm diameter, cylindrical specimens with flat surfaces polished by emery papers up to 4000 grit.

Tests were performed using a low flow rate (100mL/min) refreshed autoclave loop attached with a CER measurement system. Purity of water in the loop was controlled by using ultra-high purity ( $\sim 0.055 \mu\text{S}/\text{cm}$ ) water in the primary water tank and by purifying the effluent water from the autoclave with an ion-exchanger before flowing back into the tank. Dissolved oxygen (DO) and DH in the inlet water were controlled by bubbling either pure nitrogen gas, pure hydrogen gas or a mixture of nitrogen and hydrogen gases in the primary water tank until equilibration occurred. DO and conductivity at both inlet and outlet and DH at inlet were continuously monitored during the test. Since the test aims for clarifying the effect of DH, DO was controlled at less than 10ppb for all tests.

The principle of CER measurement as well as the experimental set-up and working principles is given in Refs. [11-12]. Briefly, the electric resistance across a solid-solid contact between two specimens exposed to the test environment is measured by passing a known value of direct current and monitoring the voltage drop. The surfaces of the two specimens were periodically contacted and disconnected at a desired time intervals. When the specimen surfaces were not in contact, they were exposed to the test environment and the surfaces were oxidized. When the specimens were brought into contact by accurate movement of a stepper motor-spring assembly, the CER was measured.

The dependence of CER on DH was measured in 288°C, pure water. One of the main concerns for varying the DH is on the DH dependent ECP, which determines whether the specimen surface is at the Ni regime, NiO regime or the Ni/NiO transition. The Ni/NiO transition can be calculated according to an equation given in Ref [13]. The initial DH used for the test was 0.9ppm at the Ni regime to ensure no NiO was formed at the start of the test. Then the DH was increased further to 1.8ppm to investigate the change of CER with DH in the Ni regime. In the following test steps the DH was decreased in sequence to 0.75 ppm (at Ni regime), 0.35ppm (around the Ni/NiO transition) and 0.16ppm and 0ppm at NiO regime.

The autoclave system used for the CER measurement was also used for the electrochemical impedance measurement in high temperature water. A Solatron 1260 impedance/gain-phase analyzer coupled with Solatron 1287 electrochemical interface over the range of 1 mHz to 30 kHz by superimposing a 0.005mA ac signal were employed for the impedance measurement. The electrode configuration used was a 2-electrodes method, i.e., the impedance response between two metal electrodes of Alloy 600 having a thin electrolyte

Table 1 Chemical composition (wt%) and mechanical properties of Alloy 600 (at room temperature)

C	Mn	Fe	S	Si	Cu	Ni	Cr	Yield strength (0.2%)	Tensile strength	Elongati on
0.07	0.37	9.46	<0.001	0.34	0.20	74.15	15.41	303MPa	696MPa	38.8%

layer was measured. This method has been employed in previous works [14]. The distance between the electrodes was controlled with an accuracy of  $10^{-7}$  m (0.1 $\mu$ m) by a step motor and was kept at 10  $\mu$ m during the measurement. Thus the tip surfaces of the two electrodes (2 mm in diameter) having a thin electrolyte layer were constructed, which enables electrochemical measurements in poorly-conductive media such as high temperature pure water.

The effects of DH on the film impedance were measured in both Ni regime and NiO regime in pure water at 250°C. At each DH level, the EIS was collected after an exposure of about 24 hrs. The procedure in changing DH during the test is summarized in Table 2.

Table 2 The DH used in each step of the impedance measurement in pure water at 250°C

Step 1	0 ppm (NiO regime)
Step 2	0.055ppm (NiO regime)
Step 3	0.2ppm (Ni regime)
Step 4	0.5ppm (Ni regime)
Step 5	1.1ppm (Ni regime)

### 3. Results and Discussion

#### 3.1. DH Dependence of the Electric Resistance of the Film

The film resistance was stabilized at about 0.7 ohm following an exposure of about six days in 288°C water at DH =0.9ppm at step 1 of CER test, Fig. 1 (a). Increasing the DH further to 1.8ppm caused an immediate decrease of film resistance to about 0.4 ohm. Similar tendency was observed in the following steps of the CER test, i.e. increase of DH reduced the film resistance and vice versa. A sharp increase of the

film resistance was observed when the DH was down to the Ni/NiO transition, implying the change of the film microstructure, Fig 1 (b). The film resistance went up to thousands ohms at DH =0, Fig. 1 (c).

The dependence of film resistance on DH observed in the test suggests that the film formed on Alloy 600 in deaerated water is a n-type semiconductor. Further, as shown in Fig 1, decreasing DH in NiO regime caused a gradual increase in film resistance before it was saturated, implying the contribution of film growth to the resistance. In the Ni regime, however, the change in the film resistance was quickly saturated following the variation of DH. The quick resistance change is very likely not a result of change in the film thickness, but an increase of the liberated electron and defects in the film due to the ionization of hydrogen in the film as will be discussed later.

#### 3.2. DH Dependence of the Electrochemical Impedance of the Film

Nyquist diagrams collected in water at 250°C at various DH levels across the Ni/NiO transition as well as the fitting using an equivalent circuit are shown in Fig. 2. The equivalent circuit shown in Fig. 3 used for the fitting was obtained based on the transfer function of the Mixed Conduction Model (MCM) model [14-16]. The equivalent circuit was developed by using transfer functions of MCM model [14]:

1) The overall impedance is the sum of the impedance of the oxide film and the oxide film/solution interface and the resistance of the solution ( $R_s$ );

2) At the oxide film/solution interface, the impedance is a parallel combination of a charge transfer resistance,  $R_{ct}$  and an interfacial capacitance,  $C_{fs}$ ;

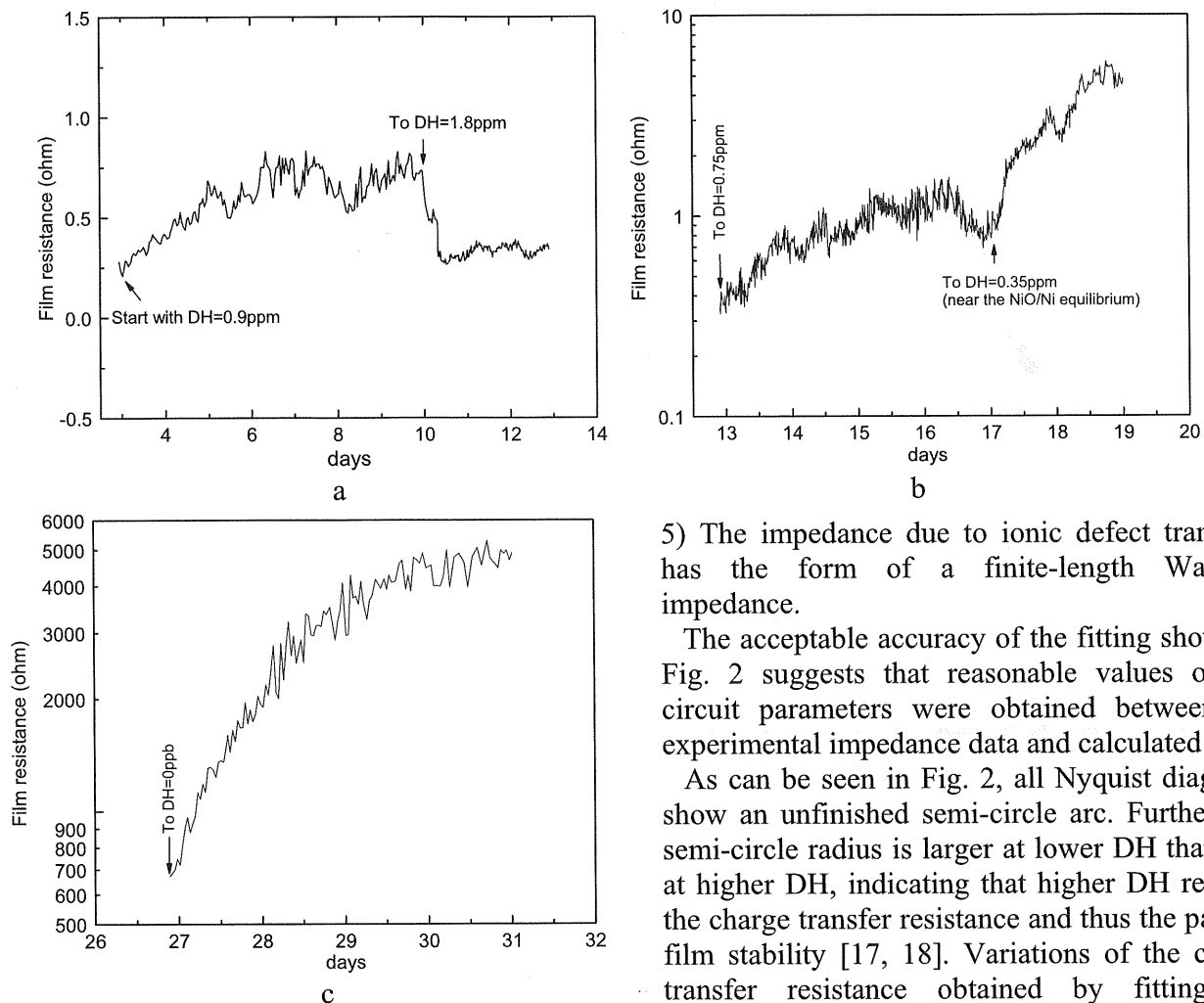


Fig. 1 CER of surface film of Alloy 600 in 288°C pure water at DH=0.9ppm and 1.8ppm (a), DH=0.75ppm and 0.35ppm (b), and DH=0ppm. (c).

3) The impedance of the oxide film is the sum of the impedances due to electronic properties (semiconductor) and the impedance of ionic defect transport;

4) The electronic contribution to the oxide film impedance can be regarded as a non-ideal capacitance of a semiconductor layer with spatially and energetically variable donor or acceptor densities, which can be approximated by a Constant Phase Element (CPE) over restricted frequency range;

5) The impedance due to ionic defect transport has the form of a finite-length Warburg impedance.

The acceptable accuracy of the fitting shown in Fig. 2 suggests that reasonable values of the circuit parameters were obtained between the experimental impedance data and calculated data.

As can be seen in Fig. 2, all Nyquist diagrams show an unfinished semi-circle arc. Further, the semi-circle radius is larger at lower DH than that at higher DH, indicating that higher DH reduces the charge transfer resistance and thus the passive film stability [17, 18]. Variations of the charge transfer resistance obtained by fitting the experiment data are shown in Fig. 4. It can be seen that increasing DH decreased the resistivity significantly, especially at the lower DH.

The decrease of the charge transfer resistance suggests the increased ionic defect transport resistance through the film or thinning of passive film by hydrogen [19]. The dependence of the ionic defect transport resistance,  $W_R$  on DH obtained by fitting the experiment data is shown in Fig. 5. Increasing DH reduced the  $W_R$  sharply in particular at lower DH levels, indicating the ionic defect transport was enhanced by higher DH.

The decrease of both  $R_{ct}$  and  $W_R$  with DH implies a large increase of protons or hydrogen atoms in the film [19]. In fact, hydrogen entered the film can be ionized and consequently the proton concentration in the film is increased [20]:

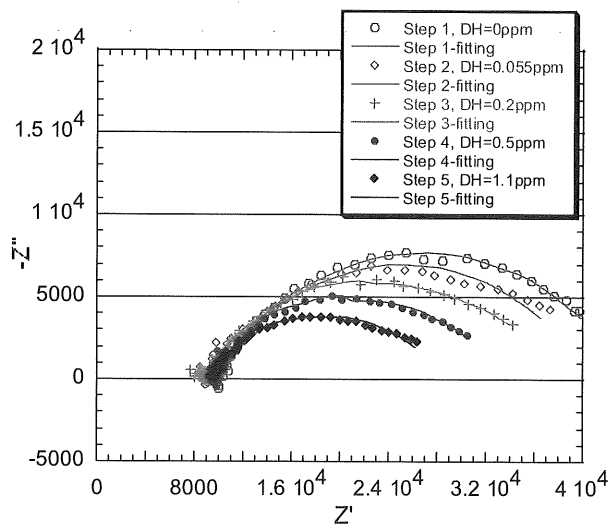


Fig. 2 The Nyquist diagrams collected in water at 250°C at various DH levels across the Ni/NiO transition and their fittings obtained by using an equivalent circuit.

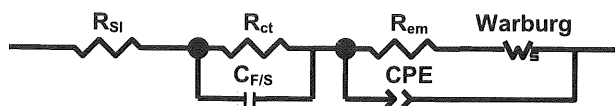
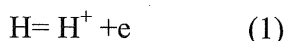


Fig. 3. The equivalent circuit used for fitting the experiment data of impedance.



Due to charge neutrality, presence of protons in the film can be expected to increase the cation vacancies, which is equivalent to enhanced cation transport. In addition, since the oxide film could generate a strong electric field across it, hydrogen protons can form a localized positive charge region due to electrostatic force between anions and protons and could also act as active sites for the ionic reactions in the film [17, 21].

In general, the dependence of  $R_{ct}$  and  $W_R$  on DH is caused by the introduction of defects and enhancement of the ionic defects transport in the film by DH in the water. Consequently, the oxidation kinetics as well as the stability of the oxide film could be changed. Further works are needed on the analysis of the DH dependences of the film stability and the thickness of each layer of the film.

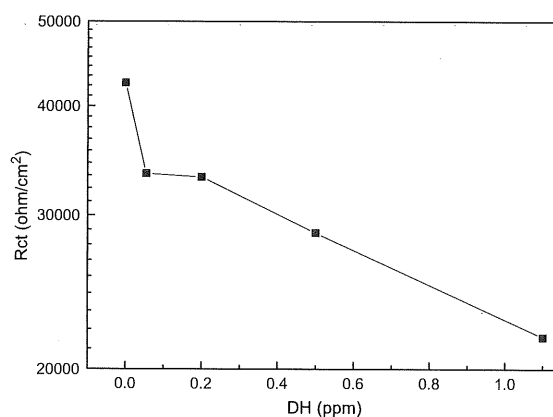


Fig. 4 The DH dependence of  $R_{ct}$  of the film formed on Alloy 600 in water at 250°C.

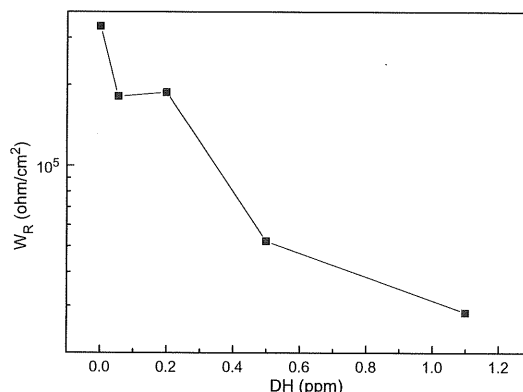


Fig. 5 The DH dependence of ionic defect transport resistance of the film formed on Alloy 600 in water at 250°C.

#### 4. Conclusions

The effects of dissolved hydrogen on the electronic properties of the film formed on Alloy 600 in high temperature water were investigated by employing the CER and impedance measurements. Dependences of the measured film resistance by CER, the charge transfer resistance and ionic defect transport resistance from impedance measurements suggest an enhanced ionic defect transport and an increase of the defects in the film, indicating the influences to the oxidation kinetics and to the stability of the oxide film.

#### 5. Acknowledgement

This research has been performed as a part of the PEACE-E program jointly supported by EDF, EPRI, Swedish Radiation Safety Authority, TEPCO, KEPCO, Tohoku-EPCO, Chubu-EPCO, JAPCO, Hitachi Ltd., MHI, Toshiba Co., and IHI.

## References

1. Q.J. Peng and T. Shoji, *Key Engineering Materials*, 261-263, 943 (2004).
2. P. Scott and P. Combrade, *Proc. 11th International Conference on Environmental Degradation of Materials in Nuclear Systems-Water Reactors*, Stevenson, WA, p.29, ANS (2003).
3. D.S. Morton, S.A. Attanasio, J.S. Fish and M.K. Schurman, *Corrosion 99*, paper 447, NACE (1999).
4. P. M Scott, *Proc. of the Ninth International Symposium on Environmental Degradation of Materials in Nuclear Power Systems-Water Reactors*, p. 3, TMS (1999).
5. D. S. Morton, S. A. Attanasio, G.A. Young, P. L. Andresen and T. M. Angeliu, *Corrosion 2001*, paper 01117, NACE (2001).
6. L. J. Qiao and J. L. Luo, *Corrosion*, 54, 281 (1998).
7. D. Wallinder, E. Hornlund and G. Hultquist, *J. of the Electrochem. Soc.*, 149, E393 (2002).
8. T. S. Mintz and T. M. Devine, *Proc. of the Twelfth International Symposium on Environmental Degradation of Materials in Nuclear Power Systems-Water Reactors*, p.873, TMS (2005).
9. P. Combrade, P. M. Scott, M. Foucault, E. Andrieu and P. Marcus, *Proc. of the Twelfth International Symposium on Environmental Degradation of Materials in Nuclear Power Systems-Water Reactors*, p. 883, TMS (2005).
10. T. Terachi, N. Totsuka, T. Yamada, T. Nakagawa, H. Deguchi, M. Horiuchi and M. Oshitani, *J. Nuclear Science and Technology*, 40, 509 (2003).
11. T. Sarrío and J. Piippo, *Materials Sci. Forum*, 185-188, 621 (1995).
12. K.S. Raja and T. Shoji, *J. of Materials Science Letters*, 22, 1347 (2003).
13. P.L. Andresen, J. Hickling, A. Ahluwalia and J. Wilson, *Presentation at the International Workshop on Optimization of Dissolved Hydrogen Content in PWR Primary Coolant*, July 18-19, 2007, Tohoku Univ., Sendai, Japan, (2007) (CD-ROM).
14. Y. Takeda, *Proc. of MIT-Tohoku "21COE" Joint Workshop on Mechanical Science based on Nanotechnology*, MIT, Cambridge, MA 02139, Mar. 12, 2008, p.24 (2008).
15. M. Bojinov, P. Kinnunen, K. Lundgren and G. Wikmarkd, *J. Electrochem. Soc.*, 152, B250 (2005).
16. M. Bojinov, G. Fabricius and T. Laitinen et al., *J. Electrochem. Soc.*, 146, 3238 (1999).
17. S. Ningshen, U. K. Mudali and G. Amarendra et al., *Corros. Sci.*, 48, 1106 (2006).
18. J.G. Yu, J.L. Luo and P.R. Norton, *Applied Surface Science*, 177, 129 (2001).
19. H. Yashiro, B. Pound, N. Kumagai and K. Tanno, *Corros. Sci.*, 40, 781 (1998).
20. T. Norby, *J. De Physique IV*, 3, 99 (1993).
21. Q. Yang L.J. Qiao, S. Chiovella and J.L. Luo, *Corrosion*, 54, 628 (1988).